Cortical Alterations in a Model for Absence Epilepsy and Febrile Seizures: In Vivo Findings in Mice Carrying a Human GABA(A)R Gamma2 Subunit Mutation

Authors

Jens Witsch MD[1,2]*; Daniel Golkowski MD[1,3]*; Thomas T. G. Hahn MD, PhD[4]; Steven Petrou PhD [5], and Hartwig Spors MD, PhD[1,6]

*Equal contribution

Affiliations

1 Max-Planck-Institute for Medical Research, Jahnstr. 29, 69120 Heidelberg, Germany

2 Department of Neurology, Columbia University College of Physicians and Surgeons, New York, USA

3 Department of Neurology, Klinikum Rechts der Isar, Technische Universität München, Munich, Germany

4 Department of Psychiatry and Systems Neurophysiology Group, Central Institute of Mental Health, Medical Faculty Mannheim of Heidelberg University, Mannheim, Germany.

5 Florey Neuroscience Institutes, University of Melbourne, Parkville, Victoria, Australia

6 Department of Neuropaediatrics, University Hospital Giessen, Feulgenstraße 10-12, 35392 Gießen, Germany

Corresponding author:

Jens Witsch, MD

Division of Critical Care Neurology, and

Comprehensive Epilepsy Center, Department of Neurology,

Columbia University, College of Physicians and Surgeons,

177 Fort Washington Avenue, Milstein 8 Center, New York, NY 10032

Phone: +1 646-355-7613; Fax: 212-305-2792; Email: jjw2167@cumc.columbia.edu

ABSTRACT

Childhood absence epilepsy (CAE) is one of the most common forms of epilepsy among children. The study of a large Australian family demonstrated that a point mutation in the gene encoding the gamma2 subunit of the GABA(A) receptor (G2R43Q) leads to an autosomal dominantly inherited form of CAE and febrile seizures (FS). In a transgenic mouse model carrying the gamma2(R43Q) mutation heterozygous animals recapitulate the human phenotype. In-vitro experiments indicated that this point mutation impairs cortical inhibition and thus increases the likelihood of seizures.

Here, using whole-cell (WC) and extracellular (EC) recordings as well as voltage-sensitive dye imaging (VSDI), we systematically searched for an in vivo correlate of cortical alterations caused by the G2R43Q mutation, as suggested by the mentioned in vitro results. We measured spontaneous and whisker-evoked activity in the primary somatosensory cortex and ventral posteriomedial nucleus of the thalamus (VPM) before and after intraperitoneal injection of the ictogenic substance pentylenetetrazol (PTZ) in urethane-anesthetized G2R43 mice and controls in a blinded setting.

Compared to wildtype controls in G2R43Q mice after PTZ injection we found 1.) Increased cortical spontaneous activity in layer 2/3 and layer 5/6 pyramidal neurons (increased standard deviation of the mean membrane potential in WC recordings), 2.) Increased variance of stimulus evoked cortical responses in VSDI experiments. 3.) The cortical effects are not due to increased strength or precision of thalamic output. In summary our findings support the hypothesis of a cortical pathology in this mouse model of human genetic absence epilepsy. Further study is needed to characterize underlying molecular mechanisms.

Keywords: Epilepsy, GABA, electrophysiology, voltage-sensitive dye imaging

INTRODUCTION

Childhood absence epilepsy (CAE) is one of the most common epilepsy syndromes mainly affecting children 4-10 years of age. Patients exhibit a sudden arrest of movements, loss of consciousness, and stereotyped hand or eye movements accompanied by 3 Hz spike-and-wave discharges (SWD) in the electroencephalogram (EEG) during seizures (Crunelli and Leresche, 2002).

“Genetic Absence Epilepsy Rats from Strasbourg“ (GAERS) and WAG/Rij rats are the two most widely used animal models for absence epilepsy (Danober et al., 1998; van Luijtelaar and Coenen, 1986). Moreover numerous gene mutations and copy number variants associated with absence epilepsy, and partly introduced in mouse models, have been found, affecting a heterogeneous group of molecular structures, for instance P/Q and T-Type calcium channels (Chen et al., 2003; Fletcher et al., 1996; Jouvenceau et al., 2001; Powell et al., 2009), voltage-

gated sodium channels (Audenaert et al., 2003; Papale et al., 2009), glutamate receptors (Bertaso et al., 2008; Beyer et al., 2008), the GLUT1 glucose transporter (Mullen et al., 2010; Suls et al., 2009), the GABA(A) receptor (Dibbens et al., 2009; Johnston et al., 2014; Kananura et al., 2002; Maljevic et al., 2006; Wallace et al., 2001) and others (Jiang et al., 2012; Muhle et al., 2011).

Research in mouse and rat models of absence epilepsy may roughly be divided in those studies, in which molecular mechanisms were investigated that supposedly cause seizures (Chipaux et al., 2011; Polack et al., 2007a; Powell et al., 2009) and those in which the epilepsy-associated network changes were explored (Carçak et al., 2014; Herd et al., 2013; Lüttjohann et al., 2013). From a clinical perspective both molecular and network investigations are equally important since they may provide new therapeutic perspectives in human patients, using pharmacological or microsurgical approaches, potentially including methods such as transcranial electrical stimulation (TES) and deep brain stimulation (DBS), which may influence aberrant network activity in specific anatomical structures (Berenyi et al., 2012; Vercueil et al., 1998). So far TMS has been used to predict responsiveness to anticonvulsive medications (Badawy et al., 2010) but therapeutic use is still experimental (Sun et al., 2012) and its effectiveness in different epilepsy syndromes remains to be shown. Deep brain stimulation (DBS), an established therapy in Parkinson's disease and other movement disorders, has been shown to terminate absence seizures in rats, in which electrodes were implanted in the subthalamic nuclei (Fisher and Velasco, 2014; Vercueil et al., 1998). However, DBS surgery in its current form seems problematic in absence epilepsy patients since they are mostly young children, and seizure frequency often spontaneously decreases over time (Camfield et al., 2014).

Here we investigated network alterations in an absence epilepsy mouse model, harboring a Arginine to Glutamine missense mutation at position 43 in the gene encoding the gamma 2 subunit of the GABA(A) receptor (G2R43Q). Initially the mutation was found in a large Australian family with the phenotypes of CAE and febrile seizures (FS) and was subsequently introduced in a transgenic mouse strain (Tan et al., 2007; Wallace et al., 2001). The resulting phenotype in heterozygous mice bears a high phenotypic and electroencephalographic similarity to affected humans making the model particularly interesting for clinically oriented investigators.

Today there is no doubt that SWDs are generated by the thalamus, the neocortex and the reciprocal neuronal connections between them (Seidenbecher et al., 1998) with some studies pointing towards a mainly cortical focus in absence epilepsy. In vitro research in G2R43Q mice as well as studies in heterozygous humans, have provided evidence supporting the theory of network alterations affecting predominantly the cortex (Fedi et al., 2008; Reid et al., 2013; Tan et al., 2007). However, so far the hypothesis of a cortical pathophysiology in

G2R43Q has not been tested in an in vivo experimental setting with thalamocortical connectivity intact.

To elucidate physiological changes caused by the G2R43Q mutation we performed voltage-sensitive dye imaging (VSDI), electrophysiological whole-cell (WC) and extracellular (EC) recordings to test the hypothesis of cortical alterations of spontaneous or evoked network activity.

RESULTS

Raw data traces and averaged data of the 3 methods used are illustrated in figure 1.

First we measured spontaneous as well as stimulus evoked neuronal activity of individual neurons (electrophysiological) as well as populations of neurons (optophysiological).

In both single-cell electrophysiological (Figure 1A+B) and cell population imaging experiments (Figure 1C) responses to a ramp-and-hold whisker stimulus were recorded before and after intraperitoneal injection of Pentylenetetrazol (PTZ) in G2R43Q mice and littermate controls, in order to assess the susceptibility to the ictogenic drug pentylenetetrazol. PTZ was administered in the dose of 40 mg/kg body weight that does not elicit overt convulsions but has been shown to evoke absence seizures in awake mice [22]. Evoked responses were recorded in form of action potentials (APs) of thalamic neurons in the ventral posteriomedial nucleus (VPM) (figure 1 A1+A2). Stimulus responses were highly reliable and occurred with a latency of <8 ms in 22 animals and with a latency of 10 ms in 2 animals. In a peri-stimulus time histogram (PSTH) from a single experiment (figure 1A2) and a PSTH from all wild-type animals pooled (suppl. figure 1) there was no apparent effect of PTZ on the base line activity before the stimulus or the reliability of the first AP, but additional APs occurred with a longer latency after PTZ administration (suppl. figure 1). AP waveforms recorded in extra-cellular configuration were not affected by the drug application (suppl. figure 1), thus automated action potential (AP) detection was possible.

In recordings from individual cortical neurons we measured stimulus evoked membrane potential depolarization (figure 1 B1) that increased after PTZ application as evident from traces averaged over 100 stimuli both before and after PTZ injection (suppl. figure 1). Cortical neurons were filled with biocytin in order to allow for anatomical reconstruction (Figure 1 B2) and in order to verify that we recorded from cortical pyramidal cells. The electrode tip positions during the recordings matched the known anatomy of the cortical layers and the position of the VPM nucleus of the thalamus (Suppl. figure 1).

In order to sample the membrane potential changes of many neurons simultaneously we performed voltage sensitive dye imaging (VSDI) experiments of the mouse barrel cortex

(figure 1 C1-2). Averaged time courses of the response amplitude illustrate the effect of PTZ (figure 1 C3).

Stronger cortical effect of PTZ on evoked activity than thalamic effect.

Impaired GABAergic inhibition increases whisker-evoked responses in cortex (Petersen et al., 2003). In order to determine where the disinhibition exerts the largest effect, we compared responses to whisker stimuli before and after systemic administration of PTZ, while recording from thalamic and cortical neurons. Figure 1 shows response rates in VPM (A3+A4), response amplitude changes of cortical layer 2/3 and 5/6 neurons (B3+B4) and amplitude changes of cortical populations responses (C3+C4). PTZ injection increased the stimulus response of thalamic and cortical neurons in both mutant and wildtype mice. Since mice with a mutation in the gamma subunit of the GABA A receptor have a lower seizure threshold when challenged with PTZ (data not shown here) we compared the PTZ effect on mutant mice and their littermate controls. Comparing 12 animals in each group (Figure 1 A4) the median number of evoked thalamic APs before PTZ-injection was 1.05±0.44 in mutant and 1.03±0.3 in wildtype mice (Mann-Whitney-U test p=0.98) and after PTZ-injection 1.15±0.64 in mutant and 1.14±0.51 in wildtype mice (p=0.89).

Comparing genotype effect in cortical layer 2/3 and 5/6 whole-cell recordings (pooled analysis of all cells) no difference in PTZ effect on the stimulus response was detected (figure 1 B4; medians: WT pre PTZ: 3.14±3.23 mV, WT post PTZ: 2.82±2.92 mV; Mann-Whitney-U-test: p=0.31). Also the variability of amplitude height, expressed as the variance of response amplitudes, did not differ significantly comparing G2R43Q mice and wildtype controls (Fisher's F-test p=0.82).

To test if subtle hyperexcitability of cortical cells would be detectable by measuring large neuronal population activity with high spatial and temporal resolution, we carried out VSDI-experiments in the mouse somatosensory cortex (Figure 1C). The variance of neuronal population response amplitudes after PTZ injection was higher in G2R43Q mice compared to wildtype controls (figure 1 C5; Fisher's F-test * p=0.04). The remaining results of the VSD experiments were in line with evoked single-cell activity: No statistically significant difference of response amplitudes was found comparing genotypes. We analyzed normalized response amplitudes by comparing ratios of four responses immediately after and four responses immediately before PTZ injection (panel C5; medians: WT post PTZ: 1.31±0.62 $*10^{-3}$ dF/F, G2R43Q post PTZ: 1.66±1.19 $*10^{-3}$ dF/F; Mann-Whitney-U test: p=0.60).

Enhanced spontaneous activity in cortex, but not in thalamus after PTZ injection in single cell recordings

In vitro studies in G2R43Q mice have shown that cortical disinhibition is subtle (Tan et al., 2007). Also, whisker-evoked responses are a product of complex interactions between cortical and subcortical brain structures, being highly dependent on stimulus timing and strength and on the state of vigilance of the animal. Thus it is conceivable that subtle alterations might not be detectable by a simple analysis of response amplitudes (Gentet et al., 2010). Furthermore we hypothesized that the increased response variance seen in the VSD recordings of whisker-evoked responses might be related to altered spontaneous cortical activity. We thus analyzed spontaneous activity (figure 2) of thalamic VPM cells (panels A1+A2), cortical layer 2/3 and 5/6 cells (B1+B2) and cortical cell populations (C1+C2).

In VPM recordings APs in a 500ms interval before-stimulation were considered spontaneous. The number of spontaneous APs did not differ between groups before PTZ (medians: WT pre PTZ: 0.005±0.6 Hz, G2R43Q pre PTZ: 0.07±0.27 Hz; *Mann-Whitney-U test p=0.53) or after PTZ injection (medians: WT post PTZ: 0.13±0.4 Hz, G2R43Q post PTZ: 0.07±2.1 Hz; **Mann-Whitney-U test p=0.79).

Cortical spontaneous activity in WC recordings was expressed as standard deviation (SD) of membrane potential changes before stimulus onset in layer 2/3 and layer 5/6 cells. Comparing the differences of SD values before and after PTZ injection between both groups (medians: WT post PTZ: 0.60±0.59 mV^2, G2R43Q post PTZ: 1.15±0.66 mV^2) revealed higher SD values in G2R43Q mutant mice after PTZ injection compared to littermate controls (figure 2 B2; Mann-Whitney-U test p=0.018)

In cortical cell population measurements using VSDI, there was no correlate of this finding on a single cell level (C1+C2). An increase of spontaneous subthreshold activity could only be seen on trend level when comparing the median responses after PTZ with the median responses before PTZ in G2R43Q mice (figure 2 C1 medians: WT pre PTZ: 0.46±0.11 $10^{-3}(dF/F)^{-2}$, WT post PTZ: 0.64±0.14 $10^{-3}x(dF/F)^{-2}$, medians: G2R43Q pre PTZ: 0.48±0.25 $10^{-3}x(dF/F)^{-2}$, G2R43Q post PTZ: 0.71±0.12 $10^{-3}x(dF/F)^{-2}$; Mann-Whitney-U-tests: ° p=0.73, °° p=0.07). Also the comparison of spontaneous activity change, i.e. the subtraction of median signal amplitudes after PTZ injection from the median signal amplitudes before PTZ injection (panel C2), between the two groups did not show a statistically significant difference between G2R43Q and control animals (figure 2 C2: medians: WT post-pre PTZ: 0.17±0.17 $10^{-3}x(dF/F)^{-2}$, G2R43Q post-pre PTZ: 0.26±0.18 $10^{-3}x(dF/F)^{-2}$,Mann-Whitney-U-test: p=0.197).

A trend towards a depolarizing membrane potential shift after PTZ in cortical cells of G2R43Q mice

To further characterize the finding of enhanced spontaneous activity in cortical layer 2/3 and layer 5/6 cells the resting membrane potential of these cells during the experiments was analyzed (figure 3). In a pooled analysis of cortical layer 2/3 and layer 5/6 cells a shift of membrane potential towards more depolarized values was observed in G2R43Q mice (figure 3B medians: G2R43Q post PTZ: 5.84±2.46 mV, n=10. This was not seen in control animals (figure 2B, medians: WT post PTZ: 2.54±3.19 mV, n=14; Mann-Whitney-U test: p=0.065).

Differential impact of G2R43Q on fast synaptic and tonic extrasynaptic inhibition?

Apart from synaptic GABA-mediated fast inhibition, the existence of extrasynaptic GABA receptors mediating so-called „tonic inhibition“ has been postulated. In cultured hippocampal cells carrying the recombinant G2R43Q receptor some results support the idea of differential impact of the mutation on phasic and tonic GABAergic inhibition (Cope et al., 2009; Eugène et al., 2007; Semyanov et al., 2004, 2003; Yagüe et al., 2013). We aimed to investigate if that might account for the discrepancy between spontaneous single cell and cell population activity.

From in vitro and in vivo VSD experiments it is known that the tangential spread of the VSD signal is dependent on intact fast synaptic inhibition and markedly increased after blockage of fast synaptic GABA receptors by the topical application of bicuculline(Laaris et al., 2000; Petersen and Sakmann, 2001). We thus analyzed the tangential spread of the cortical VSD signal calculating the area of signal expansion including all VSD image pixels with a signal intensity of >=0.75x maximum signal amplitude (figure 4 A1+A2). In all experiments included in the analysis it was manually ascertained that the maximum signal amplitude was located in projection above the D2 barrel.

We found a strong increase of the area of spread after PTZ injection in both mutant and littermate mice (figure 4C medians: WT pre PTZ: 166±102 pixels, WT post PTZ: 252±113 pixels, G2R43Q pre PTZ: 223±211 pixels, G2R43Q post PTZ: 398±163 pixels). However, there was no significant difference between mutant and littermate mice neither before (Mann-Whitney-U-Test *****p = 0.6891) nor after PTZ injection (Mann-Whitney-U-Test p = 0.3401).

DISCUSSION

In summary we found: 1.) Enhanced spontaneous single-cell activity in cortical pyramidal cells in G2R43Q mice. 2.) A membrane potential shift in these cells, which seemed to be larger in mutant than in wildtype mice, occurring in the initial phase after the PTZ-challenge and 3.) Increased variance of cortical whisker-evoked VSD amplitudes in mutant mice. 4.)

We found no effect of the genotype on whisker-evoked amplitudes in cortex in VSD and WC recordings. 5.) Our finding of a cortical membrane potential shift was not due to alterations of frequency and timing of spontaneous or evoked AP in the VPM nucleus of the thalamus.

Cortical findings

Concerning cortical findings many previous studies suggest that the mouse somatosensory cortex is likely to be the focus of absence seizure initiation (Kole et al., 2007; Meeren et al., 2002; Nersesyan et al., 2004). Therefore we conducted the VSD experiments in the somatosensory cortex, which provide data from the entire S1 region. Previous in vitro results in the G2R43Q mouse model showed, that cortical disinhibition is a very subtle feature, which is plausible from a clinical perspective, given that patients with epilepsy have normal EEG-recorded brain activity in most cases, most of the time (Tan et al., 2007). Thus our imaging finding of a trend level change of spontaneous activity in mutant G2R43Q mice may be interpreted as an in vivo correlate of this disinhibition. The fact that spontaneous activity was measured inter-ictally (simultaneous EEG recordings did not show seizure activity) and mice were anesthetized during the experiments support this hypothesis. Moreover, differences between mutant and wildtype mice might be masked by several features inherent to the VSDI technique: VSDI measures unselectively cellular signals originating from neurons of all cortical layers (dendrites from deeper layers mingle with layer 2/3 neurons) and glial cells. Thus cortical cells from the cortical surface to 200-300 μm depth contribute to the VSD signal(Ferezou et al., 2007). Most importantly, VSDI measures mean amplitudes from all cells in the imaging region. The activity of these cells is, at least interictally, largely asynchronous. Thus amplitude changes, potentially caused by the G2R43Q mutation, that we detected on single cell level, would be omitted by averaging of the VSD signal.

The membrane potential shift in cortical WC recordings after PTZ might be related to the increased spontaneous activity seen in these cells, which in turn might be a result of the interaction of the mutation and PTZ. PTZ is believed to work as an unspecific inhibitor of GABA(A) receptors, although studies about the precise PTZ effects on different subtypes of GABA(A) receptors are not available. It is known, that local application of the GABA(A) receptor antagonist gabazine leads to depolarization of cortical pyramidal cells (Mann et al., 2009). Thus it is conceivable that PTZ might have a similar depolarizing effect on pyramidal cells.

The experiments presented here were not intended to explore alterations of molecular mechanisms, caused by the G2R43Q mutation. Thus the molecular interaction between PTZ and the mutation remains speculative at this point. A hypothetical explanation is the interaction between the mutation and extrasynaptic GABA(A) receptors (Semyanov et al.,

2004). Studies have shown extrasynaptic GABAergic currents in slice preparations, that could be evoked through ambient GABA concentrations. The hypothesis that extrasynaptic GABA receptors might contribute to the stabilization of membrane potential is plausible, in that a constantly active chloride-mediated current would stabilize the membrane potential towards the reversal potential of chloride. The strength of this stabilizing effect towards a negative potential in the adult brain would depend on the one hand on the available number of involved GABA(A) receptors that mediate this current. On the other hand it would depend on the open probability of the GABA receptors. It has been speculated about an involvement of tonic inhibition in epilepsy and there are studies supporting the idea of altered tonic inhibition in the G2R43Q mouse model (Eugène et al., 2007; Semyanov et al., 2004). Nevertheless tonic inhibition is yet only described in cerebellar granule cells, dentate gyrus granule cells and hippocampal interneurons (Semyanov et al., 2004). It is also unknown which specific subunits of the GABA(A) receptors might mediate tonic inhibition. Our finding that VSD signal spread is not increased in mutant mice is in principle compatible with the idea of unimpaired fast synaptic inhibition (Laaris et al., 2000; Petersen and Sakmann, 2001). However, to date, the role of tonic inhibition in absence epilepsy is still controversial (Herd et al., 2013; Zhou et al., 2014). Further investigations are needed to test the hypothesis of a causal role of tonic inhibition in G2R4Q-related absence epilepsy.

Since evoked activity is highly dependent on ongoing spontaneous activity at the time of stimulus input (Arieli et al., n.d.; Curto et al., 2009; Petersen et al., 2003; Tsodyks et al., 1999), it is unclear why evoked activity in VSD and WC recordings was unchanged in mutant mice. A possible explanation for this finding is that increased membrane potential fluctuations will produce the same average amplitude of evoked signals as in controls, although the variance of signal amplitudes might be increased, compared to control mice.

Thalamic findings

The amplitude of cortical layer 2/3 cells in response to a sensory stimulus is driven by pronounced thalamic synchrony (Bruno and Sakmann, 2006). Cortical amplitudes in our study were not different between mutant and wildtype mice as well as before and after PTZ injection. However, to rule out an obvious influence of thalamus on our cortical findings, we carefully analyzed both spontaneous and evoked thalamic activity. This did not reveal a significant difference of the evoked or spontaneous number of APs. We observed, that also the precision of evoked APs in R43Q was not significantly different from AP precision in controls (data not shown).

To further investigate thalamocortical interactions future studies should ideally gather data from simultaneous thalamic and cortical cell pairs in vivo (Bruno and Sakmann, 2006).

Limitations of the present study

In vivo experiments are state of the art for studying many diseases. However, our experiments were carried out with mice being anesthetized. The influence of Urethane anesthesia on cortical and thalamic networks is unclear. Epileptic seizures and discharges were suppressed (as verified by EEG recordings), thus, final conclusions about seizure initiation cannot be drawn. Our study was designed to investigate single cell and cell population physiology in G2R43Q mice. If these changes are causally linked to initiation and maintenance of spike-wave-discharges needs to be investigated in a different experimental setting, dedicated to answering this question.

Furthermore the mode of action of PTZ, although being a widely used agent for seizure initiation and kindling, is not entirely understood. Thus the PTZ intervention in our experiments is unlikely to contribute to the understanding of underlying molecular mechanisms in G2R43Q mice.

CAE occurs predominantly in female patients. A similar predominance has been found in some but not all rodent models of absence epilepsy (Scharfman and MacLusky, 2014; van Luijtelaar et al., 2014). For the G2R43Q mouse no direct comparison between male and female mice has been conducted so far. Since the presented experiments were carried out in male mice, potential gender differences in G2R43Q mice need to be taken into account when interpreting the results.

Finally, thalamic and cortical measurements were not carried out simultaneously, which is necessary for the better understanding of thalamocortical network changes.

CONCLUSIONS AND OUTLOOK

Here we provide the first systematic in vivo cortical and thalamic measurements in a mouse model of human genetic childhood absence epilepsy and febrile seizures carrying a point mutation in the gamma2 subunit of the GABA(A) receptor. Our findings are compatible with previously obtained in vitro data in G2R43Q mice, that demonstrated subtly decreased inhibition in layer 2/3 cells mediated by miniature inhibitory currents (mIPSCs) (Tan et al., 2007). Moreover our results are in line with a growing body of evidence in rat models, supporting the idea of a cortical focus of pathology in absence epilepsy (Kole et al., 2007; Meeren et al., 2002; Nersesyan et al., 2004; Pinault, 2003; Polack et al., 2007b; Seidenbecher et al., 1998).

Future experiments should focus on distinct cortical circuits and cell types that might be affected by the G2R43Q mutation. For example, this might be achieved using transfection techniques to express the G2R43Q subunit only in a given structure in vivo. In a model of

conditional activation of a hypomorphic R43Q allele in adult mice the role of the mutation in developmental steps and neuronal plasticity has been assessed on a behavioral level (Chiu et al., 2008). However, these findings need to be complemented by characterization of neuronal and network alterations in vivo.

MATERIALS AND METHODS

All animal experiments were in accordance with the ethical guidelines of the Max-Planck-society and experiments were approved by the regional ethics council Karlsruhe, Baden-Württemberg, Germany.
Mice were maintained on a 12 hr light-dark cycle in isolated cages in a temperature- and humidity-controlled animal facility.

Surgical Procedures. Experiments were performed in C57Bl6 mice (G2R43Q heterozygous and wild type littermates, aged P28-P48. Mice were anaesthetized with 1.5 mg/g of Urethane intraperitoneally. The site of surgery was additionally treated with topical Lidocaine. Paw withdrawl, whisker movement and eye blink reflexes were largely suppressed. Breathing frequency and depth were observed on a regular basis and mice were continuously EKG-monitored. A heating blanket maintained the rectally measured body temperature at 37°C.
For extracellular experiments a brass pin for a stereotactical head holder (Jensen Studio, Penland, USA) was glued to the bone near lambda. For whole cell and imaging experiments a metal plate was used instead of a brass pin. For voltage-sensitive dye imaging a 3x3 mm craniotomy was produced above the barrel cortex. Craniotomy was markedly smaller in WC experiments (diameter=approx. 0.5mm). In cases of excessive brain edema, which usually happened with the larger craniotomies in imaging experiments, the cisterna magna was punctured to allow for intracranial pressure reduction. For intracranial (extracerebral) EEG recordings holes with a diameter of about 0.2mm were drilled into the skull over both hemispheres and two pieces of silver wire were carefully advanced without harming the integrity of the dura.

Electrophysiological Recordings. Intracellular and extracellular pipettes were pulled from borosilicate filamented glass on a DMZ universal puller (Zeitz Instruments, Munich, Germany). Extracellular pipettes had a long shank and 7-9 MΩ, filled with extracellular solution containing 4/5 of “F1 rat ringer” containing 138mM NaCl, 2.8 mM KCl, 2.3 mM CaCl, 2.7 mM MgCl 2.5 mM Glucose and 1/5 of PBS containing 137 mM NaCl, 2.7 mM KCl, 8 mM Na2HPO4 and 1.5 mM KH2PO4 (pH 7.1-7.2).

Extracellular recordings in the ventro-posterior medial nucleus (VPM) of the thalamus were carried out using an in vivo juxtasomal recording technique. The pipette was advanced to the region of interest. After 10 minutes, to allow time for delayed tissue movements, the pipette was advanced in 2μm steps every 2s. Increase in pipette resistance was interpreted as contact to a cell surface. VPM-cells were identified by applying a stimulus to every whisker. Cells firing on a single whisker stimulus with short latency (≤ 8ms for n=22, around 10ms for n=2) were considered VPM-cells and the principle whisker was attached to a piezoelectronic bimorph. VPM cells were typically very calm, firing only on whisker stimulation.

For WC-recordings Intrinsic imaging with a high-speed camera (Fujifilm, Tokyo, Japan) was used to localize the D2 barrel: the D2 whisker was attached to a piezoelectric bimorph and cortical responses were visualized with the camera system

Intracellular recordings were carried out using low-resistance whole cell technique as described.(Margrie et al., 2002) Patch pipettes had 5-7 MΩ. Pipettes were filled with „intracellular" solution containing: 135 mM K-Gluconat, 10 mM Hepes, 10 mM Phosphocreatin-Na, 4 mM KCl, 4 mM ATP-Mg and 0.3 mM Guanosintriphosphat. pH was adjusted to 7.2 with KOH. Series resistance was between 20 and 100MΩ during whole cell recordings. Series resistance usually slightly increased upon PTZ injection.

In whole-cell recordings resting membrane potential was defined as the 10th percentile of measured membrane potential values within the first 500 ms of each trial.

All electrophysiological recordings were conducted using an Axoclamp 2B amplifier (Axon instruments, Union City, CA, USA) and an ITC-16 (Instrutech, NY, USA). Data was acquired using an Apple Power Macintosh 7600 (Apple Inc, Cupertino, USA) with Pulse Software (HEKA Elektronik, Lamprecht, Germany) sampling extracellular traces at 50kHz and intracellular traces at 20kHz. Data were analyzed by using custom-written routines in Matlab (MathWorks).

VSDI. The dye RH1691 was applied at 0.1 mg_ml in Ringer's Solution (Optical Imaging Inc., OD A = 0.26 to 0.56 measured at 480 nm and diluting the dye solution 1:20 in ASCF) for a period of 90 minutes to the craniotomy followed by rinses to remove unbound dye. The cortex was covered with 1% agarose and a glass coverslip placed on top to minimize respiration and heartbeat-related movement artifacts. VSD signals were imaged from a focal plane 200-300 μm below the pia by using a tandem lens arrangement attached to a Fuji Deltaron HR 1700 camera (4.8 ms per frame). Excitation light was filtered with a 630-nm band pass filter, reflected onto the cortex by a 650-nm dichroic, and the epifluorescent image was collected after a 665-nm-long pass filter. Imaging data acquisition was triggered on the QRS-complex to reduce heartbeat artifacts. Experiments lasted for 5-7 hours, including

animal preparation and cortical staining, total imaging was approximately 60 minutes. Illumination was limited to the time of data acquisition, in total 3-5 minutes per animal.
For analysis imaging data were normalized to illumination (divided by the average of 4 baseline frames). Bleaching- and heartbeat-related artifacts were removed before further analysis. This was achieved by subtraction of the mean of non-stimulus trials. Response amplitudes were taken from the center of the responsive area averaged during the first 50 ms after response onset. Relative increase of response amplitudes were normalized to the average responses before PTZ-administration. Spontaneous cortical activity was determined by calculating for each animal the mean standard deviation of all camera pixel signals in all non-stimulus trials. Data were analyzed by using custom-written routines in Matlab (MathWorks).

For **Statistical Comparisons** paired or unpaired Student's t tests, Mann-Whitney U test, and one- and two-way ANOVA were used as appropriate.

Whisker Stimulation. In imaging experiments responses to single D2-whisker deflections were recorded. Stimuli were given with a piezoelectric bimorph using a 100ms ramp-and-hold waveform generated by custom-made software based on LabView (National Instruments, Austin, USA). Two stimuli of different strengths (amplitude and maximum speed of piezo deflection) were applied in random order in order to cover a larger part of the dose-response-curve. There was a 20 s pause between individual trials. In total per experiment there were 32 strong whisker stimulations, 32 weak whisker stimulations and 32 blank trials before pentylenetatrazol-injection (see below), and the same number of trials after PTZ injection. Only strong stimuli were analyzed as they produced the more stable and reproducible responses at baseline (before PTZ injection). Stimulus strengths in electrophysiological and imaging experiments were identical.
In single-cell experiments stimuli were applied through the same software and amplifier combination. Single trials lasted 1s in total. A 100ms ramp and hold stimulus was applied at t=500ms during the trial. There was a stimulus-free pause of 1s between individual trials. A train of 100 trials (duration = 200s) was started every 5 mins.

Pharmacological manipulations. To investigate effects of a disinhibiting seizure-facilitating drug on cortical population and single-cell responses in both animal groups, PTZ dissolved in saline (40 mg/kg intraperitoneally), was administered(De Deyn et al., 1992; Huang et al., 2001). In a previous study, in which EEG and fMRI measurements were combined, comparing intraperitoneal (50 mg/kg body weight) and intravenous administration of PTZ, i.p.-PTZ consistently elicited BOLD signal changes in cortex and thalamus in all animals (n=5). Signal change was most pronounced approximately 11 minutes after i.p.-PTZ

administration and correlated with spiking on EEG recordings (Keogh et al., 2005). Therefore, in our VSD-recordings, imaging was started 10 minutes after i.p.-injection of PTZ.

Reconstruction of the barrel pattern and single cell morphology. After completion of the experimental protocol the response to a second whisker stimulation was imaged for alignment of the VSD signal to the anatomical structures. Subsequently mice were cardially perfused (using 0.1M PBS followed by 4% paraformaldehyde), the brains removed and fixated with PFA and cut into 70µm-slices. Subsequent Cytochrome-C-staining made the barrel pattern and – in case of single cell experiments – the biocytin-filled cells visible (compare figure 2A), In single cell experiments this allowed the localization of the recording site and the identification of cell types. The barrel pattern and single cell morphology was then graphically reconstructed using Neurolucida software (MBF Bioscience, Williston, USA).

ACKNOWLEDGMENTS

This work was supported by the German Federal Ministry of Education and Research to Hartwig Spors (BMBF grant 01GA0504). Jens Witsch's work was supported by a research fellowship of the Max-Planck Society and by a research fellowship of the Deutsche Forschungs Gemeinschaft (Wi4300/1-1). Daniel Golkowski's work was supported by a research fellowship of the Max-Planck Society. Thomas Hahn's work was supported by the Max-Planck Society, Germany, and the German Federal Ministry of Education and Research (BMBF grants 01GQ1007 and 01GQ1003B).

Steven Petrou's work was supported by NHMRC program grant 400121 and NMHRC fellowship 1005050. The Florey Institute of Neuroscience and Mental Health is supported by Victorian State Government infrastructure funds.

We thank Bert Sakmann for his generous support and discussions during the experimental phase of the project. We thank Adi Mizrahi for cooperation and discussion and Marlies Kaiser and Ellen Stier for excellent technical assistance.

REFERENCES

Arieli, A., Sterkin, A., Grinvald, A., Aertsen, A., n.d. Dynamics of Ongoing Activity : Explanation of the Large Variability in Evoked Cortical Responses.

Audenaert, D., Claes, L., Ceulemans, B., Löfgren, A., Van Broeckhoven, C., De Jonghe, P., 2003. A deletion in SCN1B is associated with febrile seizures and early-onset absence epilepsy. Neurology 61, 854–856. doi:10.1212/01.WNL.0000080362.55784.1C

Badawy, R.A.B., Macdonell, R.A.L., Berkovic, S.F., Newton, M.R., Jackson, G.D., 2010. Predicting seizure control: Cortical excitability and antiepileptic medication. Ann. Neurol. 67, 64–73. doi:10.1002/ana.21806

Berenyi, A., Belluscio, M., Mao, D., Buzsaki, G., 2012. Closed-Loop Control of Epilepsy by Transcranial Electrical Stimulation. Science (80-.). doi:10.1126/science.1223154

Bertaso, F., Zhang, C., Scheschonka, A., de Bock, F., Fontanaud, P., Marin, P., Huganir, R.L., Betz, H., Bockaert, J., Fagni, L., Lerner-Natoli, M., 2008. PICK1 uncoupling from mGluR7a causes absence-like seizures. Nat. Neurosci. 11, 940–948. doi:10.1038/nn.2142

Beyer, B., Deleuze, C., Letts, V.A., Mahaffey, C.L., Boumil, R.M., Lew, T.A., Huguenard, J.R., Frankel, W.N., 2008. Absence seizures in C3H/HeJ and knockout mice caused by mutation of the AMPA receptor subunit Gria4. Hum. Mol. Genet. 17, 1738–1749. doi:10.1093/hmg/ddn064

Bruno, R.M., Sakmann, B., 2006. Cortex is driven by weak but synchronously active thalamocortical synapses. Science 312, 1622–7. doi:10.1126/science.1124593

Camfield, C.S., Berg, A., Stephani, U., Wirrell, E.C., 2014. Transition issues for benign epilepsy with centrotemporal spikes, nonlesional focal epilepsy in otherwise normal children, childhood absence epilepsy, and juvenile myoclonic epilepsy. Epilepsia 55 Suppl 3, 16–20. doi:10.1111/epi.12706

Carçak, N., Zheng, T., Ali, I., Abdullah, A., French, C., Powell, K.L., Jones, N.C., van Raay, L., Rind, G., Onat, F., O'Brien, T.J., 2014. The effect of amygdala kindling on neuronal firing patterns in the lateral thalamus in the GAERS model of absence epilepsy. Epilepsia 55, 654–65. doi:10.1111/epi.12592

Chen, Y., Lu, J., Pan, H., Zhang, Y., Wu, H., Xu, K., Liu, X., Jiang, Y., Bao, X., Yao, Z., Ding, K., Lo, W.H.Y., Qiang, B., Chan, P., Shen, Y., Wu, X., 2003. Association between genetic variation of CACNA1H and childhood absence epilepsy. Ann. Neurol. 54, 239–243. doi:10.1002/ana.10607

Chipaux, M., Charpier, S., Polack, P.O., 2011. Chloride-mediated inhibition of the ictogenic neurones initiating genetically-determined absence seizures. Neuroscience 192, 642–651. doi:10.1016/j.neuroscience.2011.06.037

Chiu, C., Reid, C.A., Tan, H.O., Davies, P.J., Single, F.N., Koukoulas, I., Berkovic, S.F., Tan, S.-S., Sprengel, R., Jones, M. V, Petrou, S., 2008. Developmental impact of a familial GABAA receptor epilepsy mutation. Ann. Neurol. 64, 284–293. doi:10.1002/ana.21440

Cope, D.W., Di Giovanni, G., Fyson, S.J., Orbán, G., Errington, A.C., Lorincz, M.L., Gould, T.M., Carter, D.A., Crunelli, V., 2009. Enhanced tonic GABAA inhibition in typical absence epilepsy. Nat. Med. 15, 1392–1398. doi:10.1038/nm.2058

Crunelli, V., Leresche, N., 2002. Childhood absence epilepsy: genes, channels, neurons and networks. Nat. Rev. Neurosci. 3, 371–82. doi:10.1038/nrn811

Curto, C., Sakata, S., Marguet, S., Itskov, V., Harris, K.D., 2009. A simple model of cortical dynamics explains variability and state dependence of sensory responses in urethane-

anesthetized auditory cortex. J. Neurosci. 29, 10600–12. doi:10.1523/JNEUROSCI.2053-09.2009

Danober, L., Deransart, C., Depaulis, A., Vergnes, M., Marescaux, C., 1998. PATHOPHYSIOLOGICAL MECHANISMS OF GENETIC ABSENCE EPILEPSY IN THE RAT 55.

De Deyn, P.P., D'Hooge, R., Marescau, B., Pei, Y.Q., 1992. Chemical models of epilepsy with some reference to their applicability in the development of anticonvulsants, in: Epilepsy Research. pp. 87–110. doi:10.1016/0920-1211(92)90030-W

Dibbens, L.M., Harkin, L.A., Richards, M., Hodgson, B.L., Clarke, A.L., Petrou, S., Scheffer, I.E., Berkovic, S.F., Mulley, J.C., 2009. The role of neuronal GABAA receptor subunit mutations in idiopathic generalized epilepsies. Neurosci. Lett. 453, 162–165. doi:10.1016/j.neulet.2009.02.038

Eugène, E., Depienne, C., Baulac, S., Baulac, M., Fritschy, J.M., Le Guern, E., Miles, R., Poncer, J.C., 2007. GABA(A) receptor gamma 2 subunit mutations linked to human epileptic syndromes differentially affect phasic and tonic inhibition. J. Neurosci. 27, 14108–16. doi:10.1523/JNEUROSCI.2618-07.2007

Fedi, M., Berkovic, S.F., Macdonell, R.A.L., Curatolo, J.M., Marini, C., Reutens, D.C., 2008. Intracortical hyperexcitability in humans with a GABAA receptor mutation. Cereb. Cortex 18, 664–669. doi:10.1093/cercor/bhm100

Ferezou, I., Haiss, F., Gentet, L.J., Aronoff, R., Weber, B., Petersen, C.C.H., 2007. Spatiotemporal dynamics of cortical sensorimotor integration in behaving mice. Neuron 56, 907–23. doi:10.1016/j.neuron.2007.10.007

Fisher, R.S., Velasco, A.L., 2014. Electrical brain stimulation for epilepsy. Nat. Rev. Neurol. 10, 261–70. doi:10.1038/nrneurol.2014.59

Fletcher, C.F., Lutz, C.M., Sullivan, T.N.O., Shaughnessy, J.D., Hawkes, R., Frankel, W.N., Copeland, N.G., Jenkins, N.A., Harbor, B., 1996. Absence Epilepsy in Tottering Mutant Mice Is Associated with Calcium Channel Defects 87, 607–617.

Gentet, L.J., Avermann, M., Matyas, F., Staiger, J.F., Petersen, C.C.H., 2010. Membrane potential dynamics of GABAergic neurons in the barrel cortex of behaving mice. Neuron 65, 422–35. doi:10.1016/j.neuron.2010.01.006

Herd, M.B., Brown, A.R., Lambert, J.J., Belelli, D., 2013. Extrasynaptic GABA(A) receptors couple presynaptic activity to postsynaptic inhibition in the somatosensory thalamus. J. Neurosci. 33, 14850–68. doi:10.1523/JNEUROSCI.1174-13.2013

Huang, R., Bell-horner, C.L., Dibas, M.I., Covey, D.F., Drewe, J.A., Dillon, G.H., 2001. Pentylenetetrazole-Induced Inhibition of Recombinant □ - Aminobutyric Acid Type A (GABA A) Receptors : Mechanism and Site of Action 298, 986–995.

Jiang, Y., Zhang, Y., Zhang, P., Sang, T., Zhang, F., Ji, T., Huang, Q., Xie, H., Du, R., Cai, B., Zhao, H., Wang, J., Wu, Y., Wu, H., Xu, K., Liu, X., Chan, P., Wu, X., 2012. NIPA2 located in 15q11.2 is mutated in patients with childhood absence epilepsy. Hum. Genet. 131, 1217–24. doi:10.1007/s00439-012-1149-3

Johnston, A.J., Kang, J.-Q., Shen, W., Pickrell, W.O., Cushion, T.D., Davies, J.S., Baer, K., Mullins, J.G.L., Hammond, C.L., Chung, S.-K., Thomas, R.H., White, C., Smith, P.E.M., Macdonald, R.L., Rees, M.I., 2014. A novel GABRG2 mutation, p.R136*, in a family with GEFS+ and extended phenotypes. Neurobiol. Dis. 64, 131–41. doi:10.1016/j.nbd.2013.12.013

Jouvenceau, A., Eunson, L.H., Spauschus, A., Ramesh, V., Zuberi, S.M., Kullmann, D.M., Hanna, M.G., 2001. Human epilepsy associated with dysfunction of the brain P/Q-type calcium channel. Lancet 358, 801–807. doi:10.1016/S0140-6736(01)05971-2

Kananura, C., Haug, K., Sander, T., Runge, U., Gu, W., Hallmann, K., Rebstock, J., Heils, A., Steinlein, O.K., 2002. A Splice-Site Mutation in GABRG2 Associated With Childhood Absence Epilepsy and Febrile Convulsions 59.

Keogh, B.P., Cordes, D., Stanberry, L., Figler, B.D., Robbins, C.A., Tempel, B.L., Green, C.G., Emmi, A., Maravilla, K.M., Schwartzkroin, P.A., 2005. BOLD-fMRI of PTZ-induced seizures in rats. Epilepsy Res. 66, 75–90. doi:10.1016/j.eplepsyres.2005.07.008

Kole, M.H.P., Bräuer, A.U., Stuart, G.J., 2007. Inherited cortical HCN1 channel loss amplifies dendritic calcium electrogenesis and burst firing in a rat absence epilepsy model. J. Physiol. 578, 507–25. doi:10.1113/jphysiol.2006.122028

Laaris, N., Carlson, G.C., Keller, A., 2000. Thalamic-Evoked Synaptic Interactions in Barrel Cortex Revealed by Optical Imaging 20, 1529–1537.

Lüttjohann, A., Schoffelen, J.M., van Luijtelaar, G., 2013. Peri-ictal network dynamics of spike-wave discharges: Phase and spectral characteristics. Exp. Neurol. 239, 235–247. doi:10.1016/j.expneurol.2012.10.021

Maljevic, S., Krampfl, K., Cobilanschi, J., Tilgen, N., Beyer, S., Weber, Y.G., Schlesinger, F., Ursu, D., Melzer, W., Cossette, P., Bufler, J., Lerche, H., Heils, A., 2006. A mutation in the GABA(A) receptor alpha(1)-subunit is associated with absence epilepsy. Ann. Neurol. 59, 983–987. doi:10.1002/ana.20874

Mann, E.O., Kohl, M.M., Paulsen, O., 2009. Distinct roles of GABA(A) and GABA(B) receptors in balancing and terminating persistent cortical activity. J. Neurosci. 29, 7513–7518. doi:10.1523/JNEUROSCI.6162-08.2009

Margrie, T.W., Brecht, M., Sakmann, B., 2002. In vivo, low-resistance, whole-cell recordings from neurons in the anaesthetized and awake mammalian brain. Pflugers Arch. 444, 491–8. doi:10.1007/s00424-002-0831-z

Meeren, H.K.M., Pijn, J.P.M., Luijtelaar, E.L.J.M. Van, Coenen, A.M.L., Lopes, F.H., 2002. Cortical Focus Drives Widespread Corticothalamic Networks during Spontaneous Absence Seizures in Rats 22, 1480–1495.

Muhle, H., Mefford, H.C., Obermeier, T., von Spiczak, S., Eichler, E.E., Stephani, U., Sander, T., Helbig, I., 2011. Absence seizures with intellectual disability as a phenotype of the 15q13.3 microdeletion syndrome. Epilepsia 52, e194–8. doi:10.1111/j.1528-1167.2011.03301.x

Mullen, S.A., Suls, A., De Jonghe, P., Berkovic, S.F., Scheffer, I.E., 2010. Absence epilepsies with widely variable onset are a key feature of familial GLUT1 deficiency. Neurology 75, 432–440. doi:10.1212/WNL.0b013e3181eb58b4

Nersesyan, H., Hyder, F., Rothman, D.L., Blumenfeld, H., 2004. Dynamic fMRI and EEG recordings during spike-wave seizures and generalized tonic-clonic seizures in WAG/Rij rats. J. Cereb. Blood Flow Metab. 24, 589–99. doi:10.1097/01.WCB.0000117688.98763.23

Papale, L. a, Beyer, B., Jones, J.M., Sharkey, L.M., Tufik, S., Epstein, M., Letts, V. a, Meisler, M.H., Frankel, W.N., Escayg, A., 2009. Heterozygous mutations of the voltage-gated sodium channel SCN8A are associated with spike-wave discharges and absence epilepsy in mice. Hum. Mol. Genet. 18, 1633–41. doi:10.1093/hmg/ddp081

Petersen, C.C., Sakmann, B., 2001. Functionally independent columns of rat somatosensory barrel cortex revealed with voltage-sensitive dye imaging. J. Neurosci. 21, 8435–8446. doi:21/21/8435 [pii]

Petersen, C.C.H., Hahn, T.T.G., Mehta, M., Grinvald, A., Sakmann, B., 2003. Interaction of sensory responses with spontaneous depolarization in layer 2 ¯3 barrel cortex 100.

Pinault, D., 2003. Cellular interactions in the rat somatosensory thalamocortical system during normal and epileptic 5-9 Hz oscillations. J. Physiol. 552, 881–905. doi:10.1113/jphysiol.2003.046573

Polack, P.-O., Guillemain, I., Hu, E., Deransart, C., Depaulis, A., Charpier, S., 2007a. Deep layer somatosensory cortical neurons initiate spike-and-wave discharges in a genetic model of absence seizures. J. Neurosci. 27, 6590–6599. doi:10.1523/JNEUROSCI.0753-07.2007

Polack, P.-O., Guillemain, I., Hu, E., Deransart, C., Depaulis, A., Charpier, S., 2007b. Deep layer somatosensory cortical neurons initiate spike-and-wave discharges in a genetic model of absence seizures. J. Neurosci. 27, 6590–9. doi:10.1523/JNEUROSCI.0753-07.2007

Powell, K.L., Cain, S.M., Ng, C., Sirdesai, S., David, L.S., Kyi, M., Garcia, E., Tyson, J.R., Reid, C. a, Bahlo, M., Foote, S.J., Snutch, T.P., O'Brien, T.J., 2009. A Cav3.2 T-type calcium channel point mutation has splice-variant-specific effects on function and segregates with seizure expression in a polygenic rat model of absence epilepsy. J. Neurosci. 29, 371–80. doi:10.1523/JNEUROSCI.5295-08.2009

Reid, C. a, Kim, T., Phillips, a M., Low, J., Berkovic, S.F., Luscher, B., Petrou, S., 2013. Multiple molecular mechanisms for a single GABAA mutation in epilepsy. Neurology 80, 1003–8. doi:10.1212/WNL.0b013e3182872867

Scharfman, H.E., MacLusky, N.J., 2014. Sex differences in the neurobiology of epilepsy: A preclinical perspective. Neurobiol. Dis. doi:10.1016/j.nbd.2014.07.004

Seidenbecher, T., Staak, R., Pape, H., 1998. Relations between cortical and thalamic cellular activities during absence seizures in rats 10, 1103–1112.

Semyanov, A., Walker, M.C., Kullmann, D.M., 2003. GABA uptake regulates cortical excitability via cell type-specific tonic inhibition. Nat. Neurosci. 6, 484–490. doi:10.1038/nn1043

Semyanov, A., Walker, M.C., Kullmann, D.M., Silver, R.A., 2004a. Tonically active GABAA receptors: Modulating gain and maintaining the tone. Trends Neurosci. doi:10.1016/j.tins.2004.03.005

Semyanov, A., Walker, M.C., Kullmann, D.M., Silver, R.A., 2004b. Tonically active GABA A receptors: modulating gain and maintaining the tone. Trends Neurosci. 27, 262–9. doi:10.1016/j.tins.2004.03.005

Suls, A., Mullen, S.A., Weber, Y.G., Verhaert, K., Ceulemans, B., Guerrini, R., Wuttke, T. V, Salvo-Vargas, A., Deprez, L., Claes, L.R.F., Jordanova, A., Berkovic, S.F., Lerche, H., De Jonghe, P., Scheffer, I.E., 2009. Early-onset absence epilepsy caused by mutations in the glucose transporter GLUT1. Ann. Neurol. 66, 415–419. doi:10.1016/S0513-5117(09)79174-4

Sun, W., Mao, W., Meng, X., Wang, D., Qiao, L., Tao, W., Li, L., Jia, X., Han, C., Fu, M., Tong, X., Wu, X., Wang, Y., 2012. Low-frequency repetitive transcranial magnetic stimulation for the treatment of refractory partial epilepsy: a controlled clinical study. Epilepsia 53, 1782–9. doi:10.1111/j.1528-1167.2012.03626.x

Tan, H.O., Reid, C.A., Single, F.N., Davies, P.J., Chiu, C., Murphy, S., Clarke, A.L., Dibbens, L., Krestel, H., Mulley, J.C., Jones, M. V, Seeburg, P.H., Sakmann, B., Berkovic, S.F., Sprengel, R., Petrou, S., 2007. Reduced cortical inhibition in a mouse model of familial childhood absence epilepsy. Proc. Natl. Acad. Sci. U. S. A. 104, 17536–17541. doi:10.1073/pnas.0708440104

Tsodyks, M., Kenet, T., Grinvald, A., Arieli, A., 1999. Linking spontaneous activity of single cortical neurons and the underlying functional architecture. Science 286, 1943–1946. doi:10.1126/science.286.5446.1943

Van Luijtelaar, E.L., Coenen, A.M., 1986. Two types of electrocortical paroxysms in an inbred strain of rats. Neurosci. Lett. 70, 393–397. doi:10.1016/0304-3940(86)90586-0

Van Luijtelaar, G., Onat, F.Y., Gallagher, M.J., 2014. Animal models of absence epilepsies: what do they model and do sex and sex hormones matter? Neurobiol. Dis. doi:10.1016/j.nbd.2014.08.014

Vercueil, L., Benazzouz, A., Deransart, C., Bressand, K., Marescaux, C., Depaulis, A., Benabid, A.L., 1998. High-frequency stimulation of the sub-thalamic nucleus suppresses absence seizures in the rat: Comparison with neurotoxic lesions. Epilepsy Res. 31, 39–46. doi:10.1016/S0920-1211(98)00011-4

Wallace, R.H., Marini, C., Petrou, S., Harkin, L.A., Bowser, D.N., Panchal, R.G., Williams, D.A., Sutherland, G.R., Mulley, J.C., Scheffer, I.E., Berkovic, S.F., 2001. Mutant GABA(A) receptor gamma2-subunit in childhood absence epilepsy and febrile seizures. Nat. Genet. 28, 49–52. doi:10.1038/88259

Yagüe, J.G., Cavaccini, A., Errington, A.C., Crunelli, V., Di Giovanni, G., 2013. Dopaminergic modulation of tonic but not phasic GABAA-receptor-mediated current in the ventrobasal thalamus of Wistar and GAERS rats. Exp. Neurol. 247, 1–7. doi:10.1016/j.expneurol.2013.03.023

Zhou, C., Ding, L., Deel, M.E., Ferrick, E.A., Emeson, R.B., Gallagher, M.J., 2014. Altered intrathalamic GABAA neurotransmission in a mouse model of a human genetic absence epilepsy syndrome. Neurobiol. Dis. 73C, 407–417. doi:10.1016/j.nbd.2014.10.021

FIGURE LEGENDS

Figure 1
Whisker-evoked activity in thalamic extracellular (A), cortical whole-cell- (B) and VSD-recordings (C) is not increased in G2R43Q mice.
(A) Thalamic action potential (AP) responses to a 100 ms ramp-and-hold stimulus at 0.5 Hz. (A1) Example trace from a wildtype (WT) mouse sampled at 50 kHz. (A2) PSTH from a single animal showing average number of APs per trial from the example in (A) with 5 ms binning. Blue: average PSTH from 200 stimuli before PTZ injection. Cyan: PSTH from 300 stimuli 10-20 mins after PTZ injection. (A3) Median evoked APs per stimulus averaged from 100 trials (bars: SEM) during the course of experiments. t=0: time of PTZ injection. (A4) Average evoked APs in single animals before and 10-20 mins after PTZ injection (also indicated by grey overlay boxes in A3). Crosses represent single experiments.
(B1) Example traces from intracellular recordings in a cortical pyramidal neuron of a WT mouse both before and after PTZ injection together with the 100 ms ramp-and-hold stimulus. The rectangular overlay indicates the time window in which the amplitude is calculated. (B2) Reconstructed layer 2/3 pyramidal neuron. Left: projection from above, right: from the side. Dendritic arbor shown in blue, axon in red. Soma is located above barrel D2. (B3) Effect of PTZ on stimulus response amplitude in pooled layer 2/3 and 5/6 cells (each cell different animal) normalized to mean amplitude before PTZ. Mean depolarization in an average from 100 sweeps within a 50 ms post stimulus time-window (also indicated by grey overlay boxes in Figure 1 E and F). (B4) Change of average depolarization for 5-10 minutes after PTZ injection in all animals normalized to mean before PTZ.
(C) Voltage-sensitive dye imaging of whisker-evoked responses in the mouse primary somatosensory cortex (S1)/barrel cortex
(C1) VSD signal dF/F increase after PTZ administration in an example G2R43Q mouse. Map average of 32 repetitions. Left: “Green” image showing the blood vessel pattern of the barrel cortex region. (C2) Schematic of the barrel system pathway: trigeminal neuron, brainstem neuron, VPM neuron. The latter projects to cortical layer 4, barrel cortex. Light microscopy image: cytochrome-C-stained tangential section of the mouse barrel cortex.
Drawing in from Feldman DE and Brecht M, 2005, Science, 310(5749):810-815. Reprinted with permission from AAAS. (C3) Averaged response traces (32 repetitions) of the same animal before (red) and after (magenta) PTZ. The rectangular overlay indicates the time window (50 ms) in which the mean amplitude was calculated. (C4-C5) Mean of VSD response amplitudes (dF/F) normalized to mean before PTZ injection. Response amplitudes calculated in the center pixels of the responsive area. Each data point mean of 8 whisker stimulations times number of animals. (C4) Time course of response amplitudes relative to PTZ i.p.-injection. (C5) Average of 4 cortical response amplitudes immediately before versus after PTZ (each data point represents mean of 4 responses in one animal respectively). * indicates significant difference of variance (F-test p=0.04).

Figure 2
Higher spontaneous activity in cortical pyramidal cells in G2R43Q compared to littermates.
(A1) Median spontaneous AP frequency of all VPM cells recorded during the course of

experiments. 100 trials were averaged per time point (bars: SEM). t=0: time of PTZ injection. (A2) Mean spontaneous firing frequency in WT and R43Q animals (values averaged from grey overlay boxes in (A1)). Crosses represent single experiments. Black lines connect paired data points. (B1) Spontaneous activity of all animals as single data points. Mean SD values of the first 500 ms of 100 recorded traces per data point both before and 5-10 minutes after PTZ injection. (B2) Change of spontaneous activity 5-10 minutes after PTZ injection. Crosses represent single animals. G2R43Q n=10, WT n=14. (C1) Spontaneous VSD cortical activity plotted as average standard deviation of the VSD signal (dF/F) of all pixels of all camera frames of all trials in one animal both before and after PTZ injection. Black lines connect paired data points. ***** Fisher's test: p=0.0006, mutant vs. WT post PTZ Fisher's test: p= 0.42; G2R43Q n=23, WT n=24. (C2) Change of spontaneous activity after PTZ. Values normalized to spontaneous mean SD before PTZ injection. Crosses represent average values of single animals.

Figure 3

Membrane potential shift of cortical pyramidal cells after PTZ higher in G2R43Q.

(A) Normalized median resting membrane potential: errorbar plot showing median of all animals with standard error. The 10^{th} percentile of membrane potential values within the first 500 ms of each recorded trace was considered as resting membrane potential. Average of 100 traces per data point. Individual cells were normalized to pre PTZ values. (B) Increase of membrane potential 5-10 minutes after PTZ administration. Crosses represent single animals. G2R43Q n=10, WT n=14.

Figure 4

PTZ increases the area of spread of the cortical VSD signal in both groups, but not more in G2R43Q mice.

Tangential spread of voltage-sensitive dye signal within somatosensory cortex layer 2/3. (A1)+(A2) Example maps of 4 averaged whisker-evoked cortical responses each, normalized to the region of maximum response within a time window of 96 ms (20 camera frames) after response onset. The area of spread (encircled by white line) includes all image pixels with a response magnitude >=0.75 x maximum response. Color bar: Signal amplitude normalized to maximum. (B) Time course of mean signal spread relative to PTZ injection. Each data point mean of 8 whisker stimulations x number of animals. (C) Mean spread of VSD signal shown for each animal included in (B). Each data point mean of 4 whisker stimuli before and after PTZ injection respectively.

Supplementary Figure 1

Thalamic (VPM) extracellular (A) and cortical layer 2/3 and 5/6 whole-cell (B) data acquisition and binning

Thalamic action potential (AP) responses to a 100 ms ramp-and-hold stimulus at 0.5 Hz. (A1) Example traces from a wildtype (WT) mouse sampled at 50 kHz. (A2) PSTH from a single animal showing average number of APs per trial from the example in (A) with 5 ms binning. Blue: average PSTH from 200 stimuli before PTZ injection. Cyan: PSTH from 300 stimuli 10-20 mins after PTZ injection. (A3) PSTHs showing the average number of APs per trial from all WT animals (n=12) with 5 ms binning both before and after PTZ administration.

(A4) All APs detected in a complete experiment superimposed together with autocorrelation plots of all detected APs superimposed. Note the uniformity of APs and 2 ms absolute refractory time supporting that only a single neuron was recorded.

(B1) Example traces from intracellular recordings in a cortical pyramidal neuron of a WT mouse both before and after PTZ injection together with the 100 ms ramp-and-hold stimulus. The rectangular overlay indicates the time window in which the amplitude is calculated.(B2) Average of 100 stimuli before and after PTZ injection in a WT animal (cells from layer 2/3 n=11, layer 5/6 n=3). (B3) Reconstructed layer 2/3 pyramidal neuron. Left: projection from above, right: from the side. Dendritic arbor shown in blue, axon in red. Soma is located above barrel D2. (B4) Mean recording depth in VPM, L2/3 and L5/6 cells.

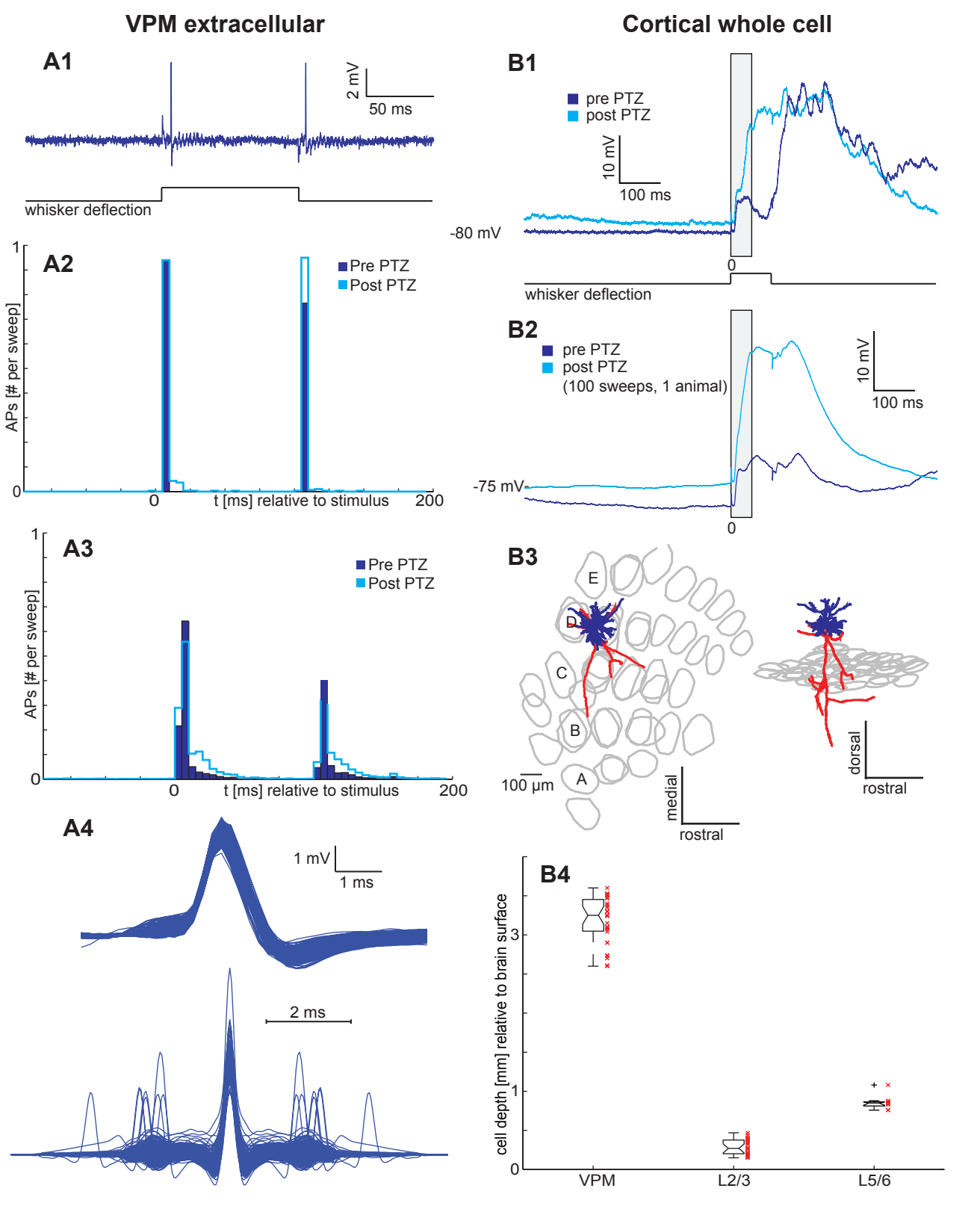
VPM extracellular
Cortical whole cell
A1
2 mV
50 ms
whisker deflection
A2
Pre PTZ
Post PTZ
APs [# per sweep]
t [ms] relative to stimulus
A3
Pre PTZ
Post PTZ
APs [# per sweep]
t [ms] relative to stimulus
A4
1 mV
1 ms
2 ms
B1
pre PTZ
post PTZ
10 mV
100 ms
-80 mV
whisker deflection
B2
pre PTZ
post PTZ
(100 sweeps, 1 animal)
10 mV
100 ms
-75 mV
B3
E
D
C
B
A
100 µm
medial
rostral
dorsal
rostral
B4
cell depth [mm] relative to brain surface
VPM
L2/3
L5/6

VPM extracellular

A1

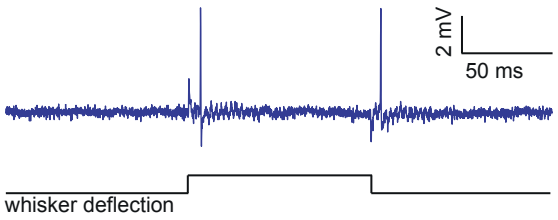

A2

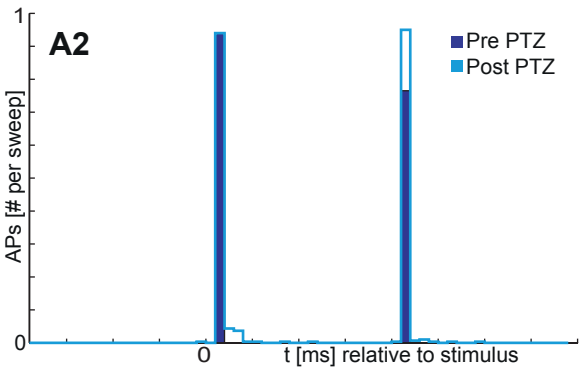

A3

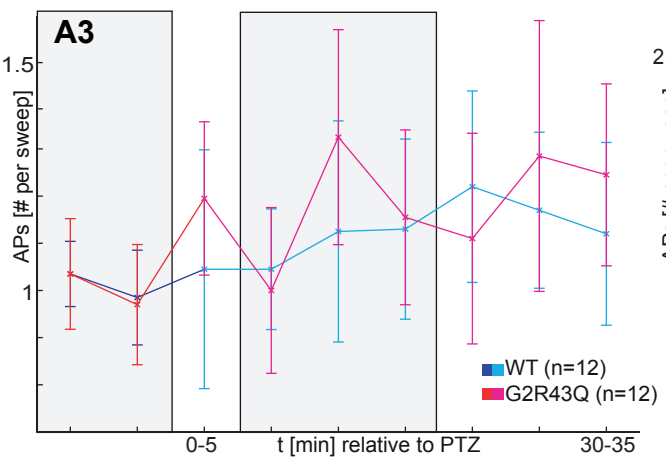

A4

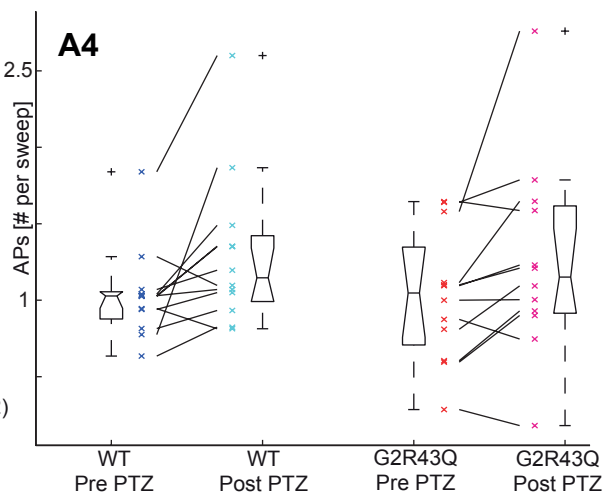

Cortical whole cell

B1

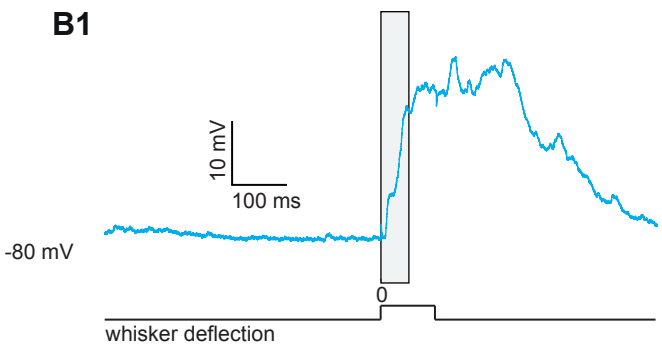

B2

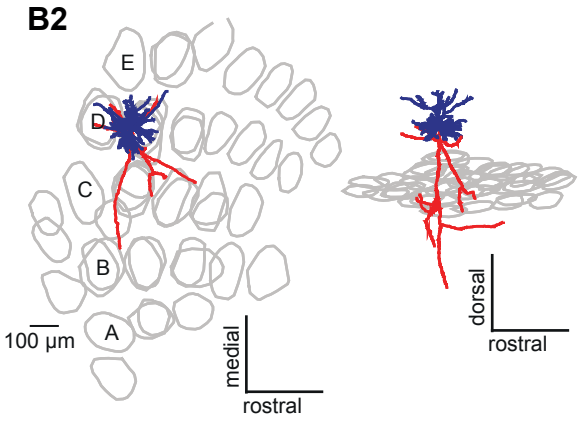

B3

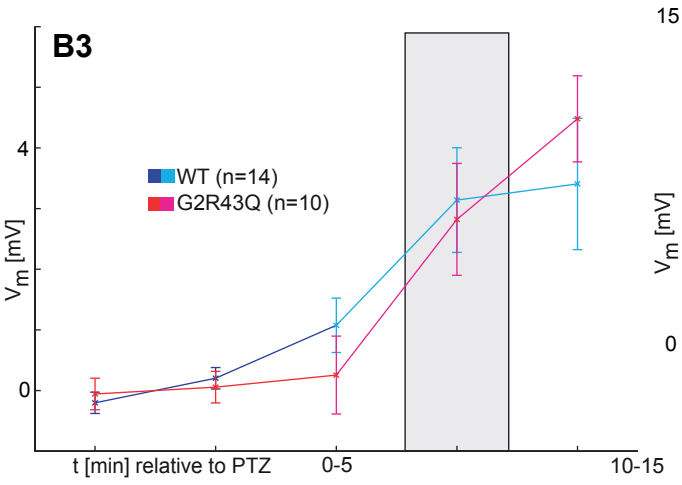

B4

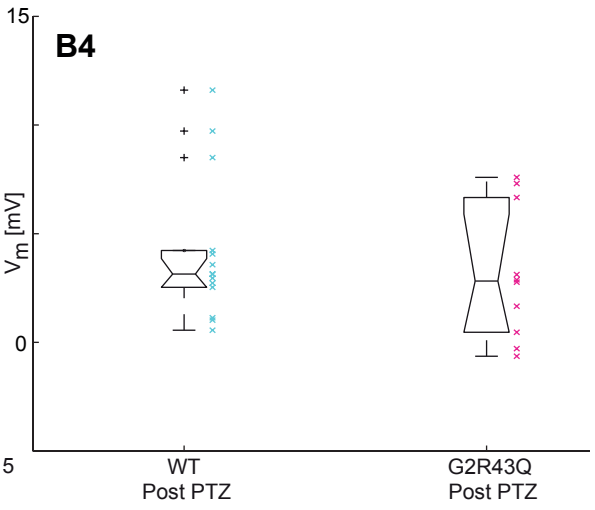

Cortical VSD-Imaging

C1

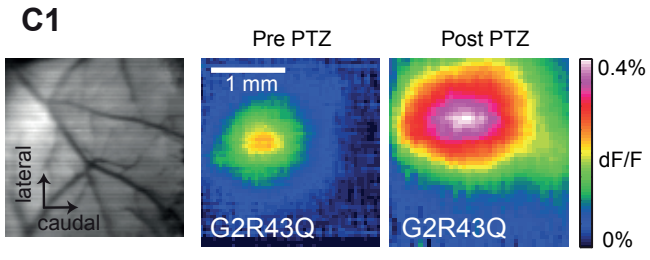

C2

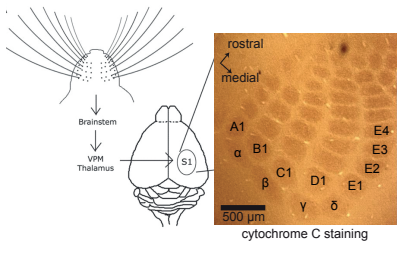

C3

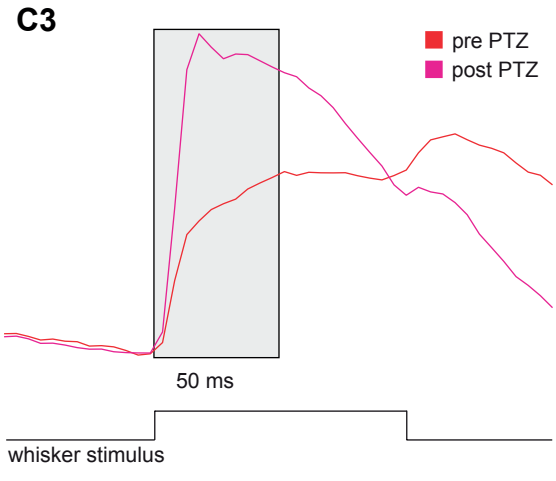

C4

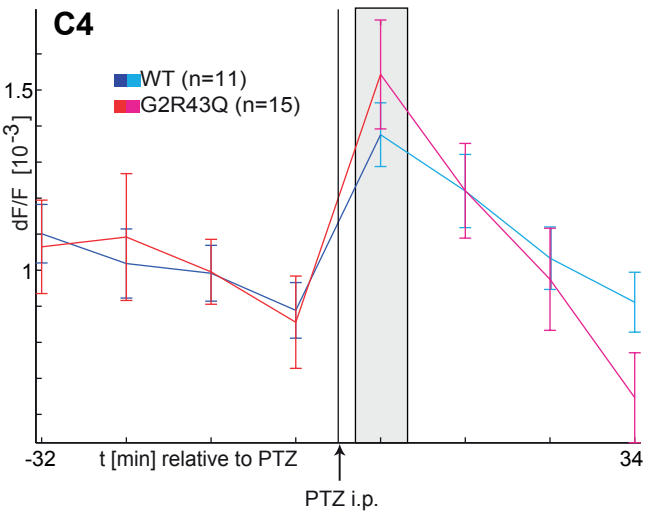

C5

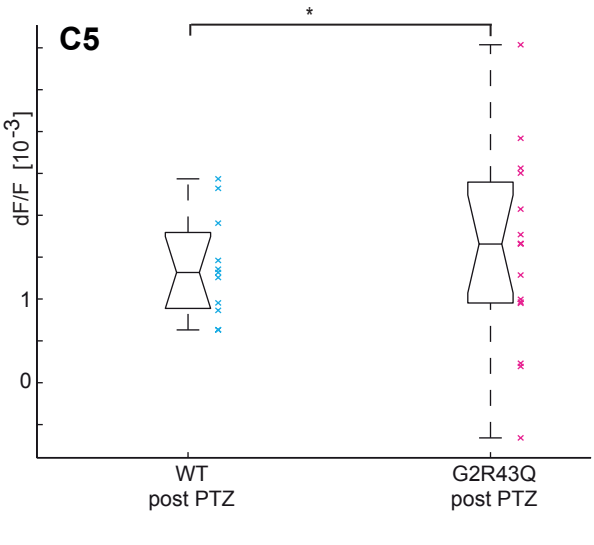

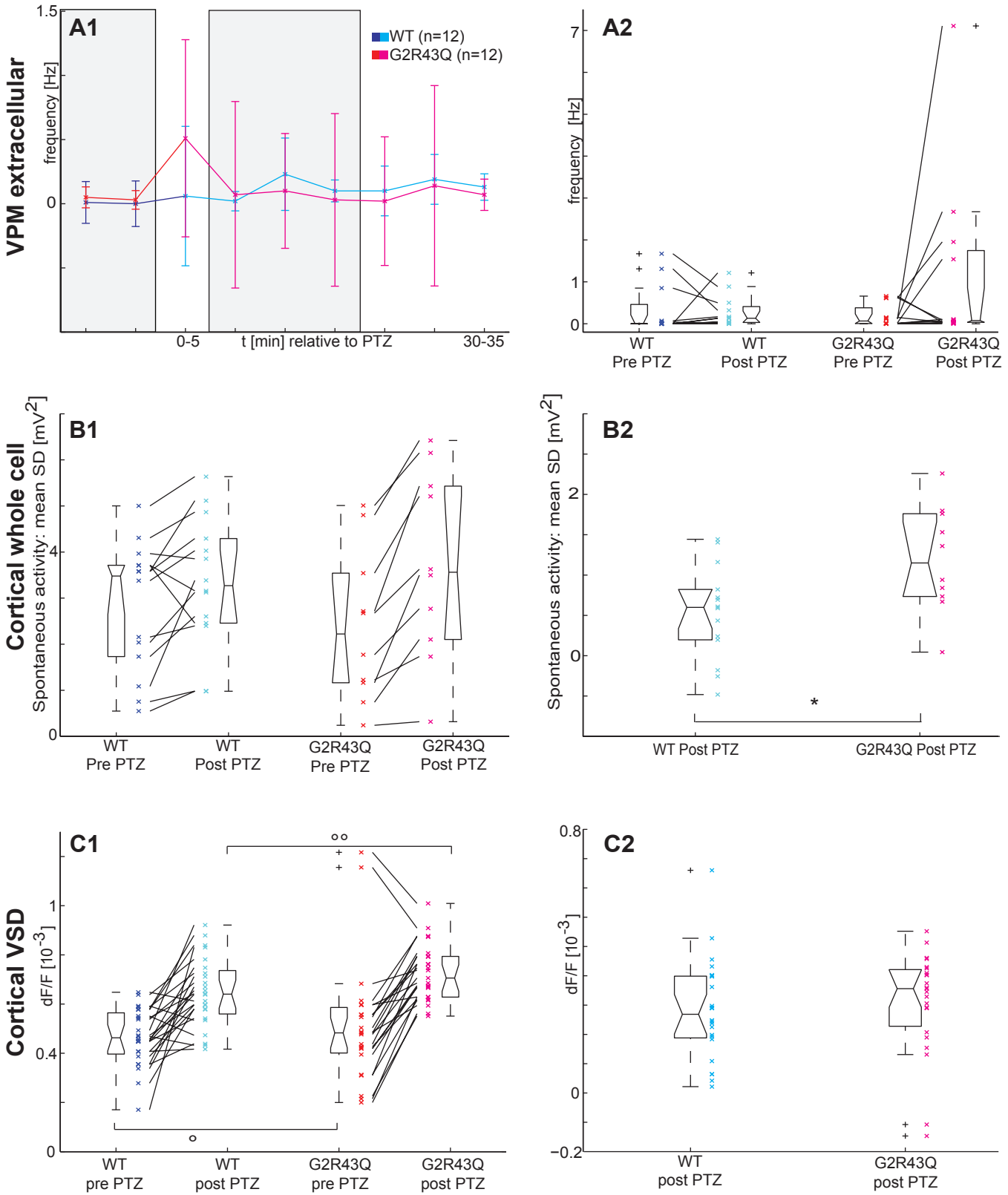
A1
VPM extracellular
frequency [Hz]
1.5
0
WT (n=12)
G2R43Q (n=12)
0-5
t [min] relative to PTZ
30-35
A2
frequency [Hz]
7
1
0
WT Pre PTZ
WT Post PTZ
G2R43Q Pre PTZ
G2R43Q Post PTZ
B1
Cortical whole cell
Spontaneous activity: mean SD [mV2]
4
0
WT Pre PTZ
WT Post PTZ
G2R43Q Pre PTZ
G2R43Q Post PTZ
B2
Spontaneous activity: mean SD [mV2]
2
0
*
WT Post PTZ
G2R43Q Post PTZ
C1
Cortical VSD
dF/F [10-3]
1
0.4
0
WT pre PTZ
WT post PTZ
G2R43Q pre PTZ
G2R43Q post PTZ
C2
dF/F [10-3]
0.8
0
−0.2
WT post PTZ
G2R43Q post PTZ

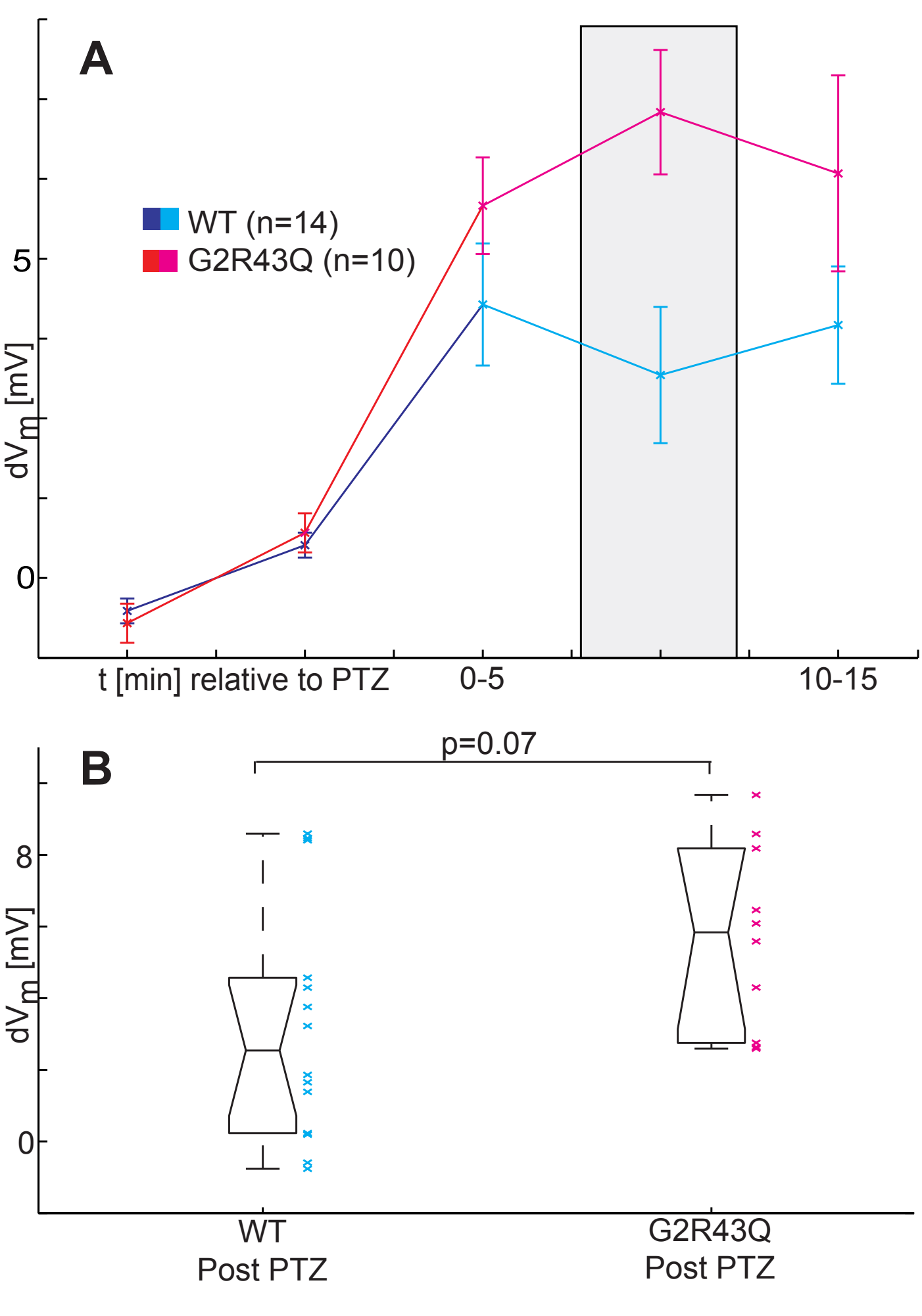
A
WT (n=14)
G2R43Q (n=10)
5
0
dVm [mV]
t [min] relative to PTZ
0-5
10-15
B
p=0.07
8
0
dVm [mV]
WT
Post PTZ
G2R43Q
Post PTZ

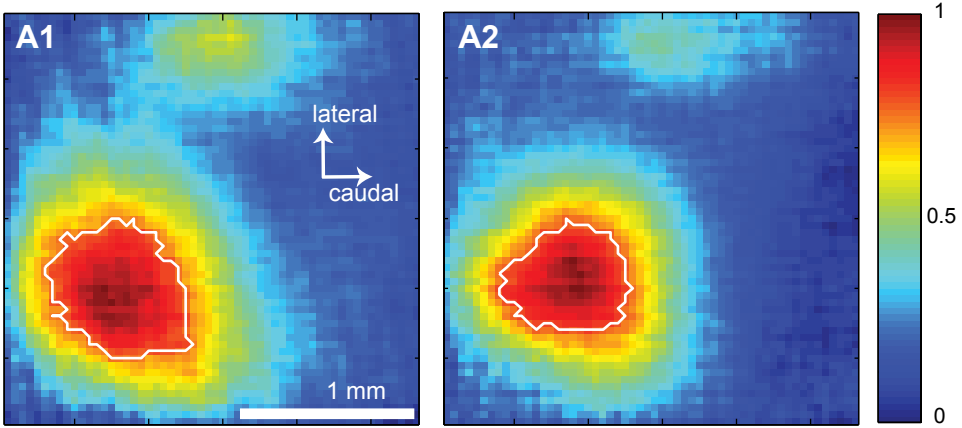
A1
lateral
caudal
1 mm
A2
1
0.5
0

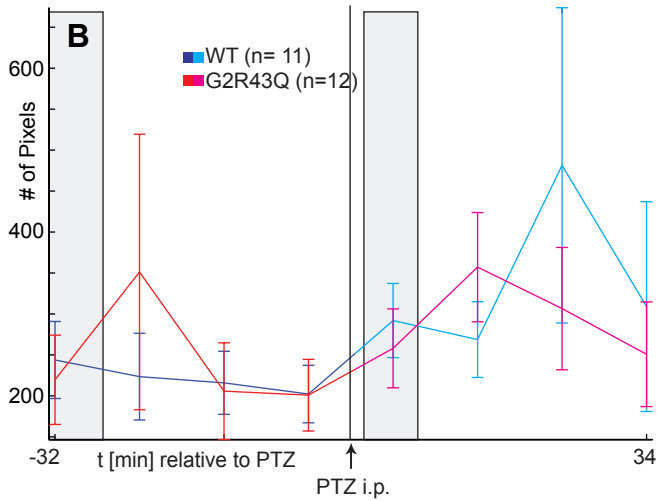
B
WT (n= 11)
G2R43Q (n=12)
600
400
200
# of Pixels
-32
t [min] relative to PTZ
34
PTZ i.p.

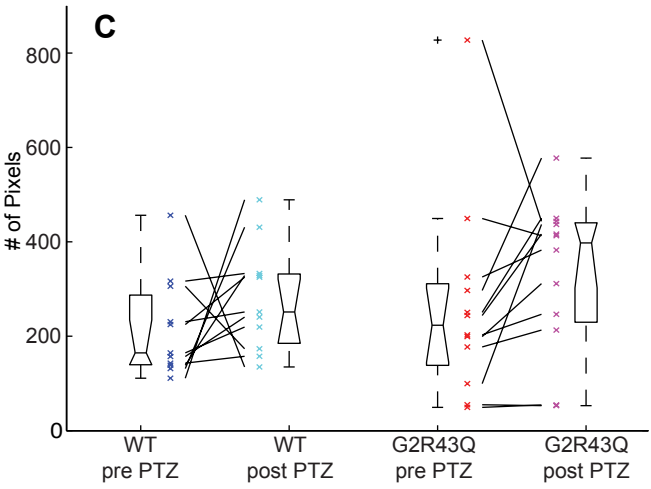
C
800
600
400
200
0
# of Pixels
WT
pre PTZ
WT
post PTZ
G2R43Q
pre PTZ
G2R43Q
post PTZ

Author/s:
Witsch, J; Golkowski, D; Hahn, TTG; Petrou, S; Spors, H

Title:
Cortical alterations in a model for absence epilepsy and febrile seizures: In vivo findings in mice carrying a human GABA(A)R gamma2 subunit mutation

Date:
2015-05-01

Citation:
Witsch, J; Golkowski, D; Hahn, TTG; Petrou, S; Spors, H, Cortical alterations in a model for absence epilepsy and febrile seizures: In vivo findings in mice carrying a human GABA(A)R gamma2 subunit mutation, NEUROBIOLOGY OF DISEASE, 2015, 77 pp. 62 - 70